Supporting Information

A Five-Coordinate Ni(I) Complex Supported by 1,4,7-Triisopropyl-1,4,7-triazacyclononane

Leonel Griego,[‡] Toby J. Woods,[‡] and Liviu M. Mirica[*,‡]

[‡]Department of Chemistry, University of Illinois at Urbana−Champaign, 600 South Mathews Avenue, Urbana, Illinois 61801, United States

E-mail: mirica@illinois.edu

Table of Contents

I. General specifications 2
II. Synthesis of Complexes Supported by iPr_3TACN 3
Synthesis of $(iPr_3TACN)Ni^{II}Cl_2$ 3
Synthesis of $(iPr_3TACN)Ni^{II}Me_2$ 4
Synthesis of $[(iPr_3TACN)Ni^{II}NO]PF_6$ 5
Synthesis of $[(iPr_3TACN)Ni^{II}(MeCN)_2](PF_6)_2$ 6
Synthesis of $[(iPr_3TACN)Ni^{II}(CN^tBu)_3](PF_6)_2$ 7
Synthesis of $[(iPr_3TACN)Ni^{I}(CN^tBu)_2]PF_6$ 8
III. NMR Spectra 9
IV. IR Spectra 10
IV. Cyclic Voltammetry Experiments 12
V. UV-Vis Spectra 13
VI. EPR Spectra and Simulations of Ni^I Complex 15
VIII. DFT Calculations 17
IX. X-ray Structure Determinations of $(iPr_3TACN)Ni$ Complexes 19
X. References 37

I. General specifications

All experiments were carried out under a nitrogen atmosphere using standard glove box and/or Schlenk techniques. Reagents for which the synthesis is not given were commercially available from Sigma Aldrich, Acros, or STREM, and were used without further purification. Solvents used were purified prior to use by passing through a column of activated alumina or molecular sieves using an MBRAUN solvent purification system. The 1,4,7-triazacyclononane (TACN) ligand precursors and final ligand were synthesized from previously reported procedures.[1-4] Varian 500 MHz instrument was used to collect NMR data. Chemical shifts are reported in ppm with the residual solvent peak as the reference. Abbreviations for NMR and IR multiplicity are s (singlet), d (doublet), t (triplet), and m (multiplet). Solid-state infrared spectra were measured using a PerkinElmer Frontier FT-IR spectrophotometer equipped with a KRS5 thallium bromide/iodide universal attenuated total reflectance accessory. UV-visible spectra were recorded on a Varian Cary 50 Bio spectrophotometer. EPR spectra were recorded using a Bruker 10" EMXPlus X-band Continuous Wave EPR spectrometer at 77 K. GC-MS data was collected using an Agilent 7890B GC Series System and an Agilent 5977B Mass Selective Detector. Electrospray ionization mass spectrometry (ESI-MS) was recorded on a Water Q-TOF Ultima ESI instrument by the Mass Spectrometry Laboratory at the University of Illinois at Urbana−Champaign (UIUC). Elemental analysis was carried out by the Microanalysis Laboratory at UIUC using an Exeter Analytical - Model CE440 CHN Analyzer. Magnetic moments were calculated using the Evans method for a known concentration of the metal complex, with a sealed capillary containing the desired solvent.[5-6] Cyclic voltammetry (CV) was performed using a BASi EC Epsilon electrochemical workstation or a CHI Electrochemical Analyzer 660D. Measurements were taken in a glove box under nitrogen. Glassy carbon disk electrode (d = 1.6 mm) was used as the working electrode for cyclic voltammetry and the auxiliary electrode was a platinum wire. A Ag wire was used as the reference electrode. The reference was calibrated against ferrocene after each experiment. The geometry index was calculated based on published procedures and represented as tau (τ).[7-8]

II. Synthesis of Complexes Supported by iPr_3TACN

Synthesis of $(iPr_3TACN)Ni^{II}Cl_2$

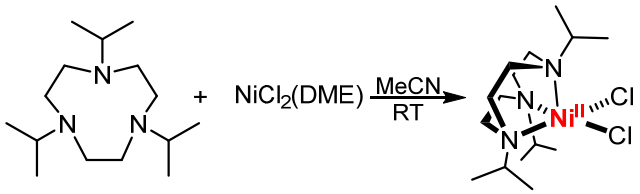

The tri-isoproypyl-1,4,7-triazacyclononane ligand (0.8 g, 3.1 mmol) was dissolved in 10 mL of a mixture of MeCN/Et_2O (10:1). The $NiCl_2$(DME) (0.69 g, 3.1 mmol) was added as an orange solid to the stirring ligand solution. The solution changed to a green color as a yellow precipitate formed overtime. Allowed to stir overnight. A dark yellow powder stirred in a green solution (presumably the monohalide with a coordinated acetonitrile). Approximately 5 mL of Et_2O were added to the solution as the green color faded and more yellow powder precipitated. The precipitate was collected, washed with Et_2O, and dried under vacuo. Crystals suitable for X-ray crystallography were grown using through vapor diffusion of Et_2O in a concentrated solution of MeCN at -35 ºC. Yield: 1.1 g, 91%.

Characterization of this complex was identical those previously reported.[9-10]

Synthesis of ($iPr_3TACN)Ni^{II}Me_2$

($iPr_3TACN)NiCl_2$ (385 mg, 1 mmol) was suspended in 10 mL of Et_2O and cooled to -35 ºC in a $N_{2\,(g)}$ glovebox. A solution of 3.0 M of MeMgCl in THF (667 µL, 2 mmol) was then added as a colorless liquid to the cold stirring suspension. The color quickly changed to a dark yellow with an off-white precipitate as the ($iPr_3TACN)NiCl_2$ reacted for 3 hours at -35 ºC. The solution was filtered through a small Celite column and solution was collected. All solvents were removed under vacuum to obtain a crude dark yellow-brown solid. The product was then extracted using cold pentane and filtered through a small Celite column to collect a clear yellow filtrate. Removal of all volatiles at -35 ºC afforded a crystalline yellow powder. Crystals suitable for X-ray crystallography were grown in a concentrated solution of Et_2O at -35 ºC. Yield: 241 mg, 70%.

NMR: ^{1}H-NMR (500 MHz, CD_3CN, -20 ºC), δ (ppm): 2.79 (sept, 3H, CH), 2.58 (s, 12H, -CH_2-), 0.94 (d, 18H, -CH_3), 0.90 (s, 6H, Ni-CH_3).

^{13}C-NMR (500 MHz, CD_3CN, -20 ºC), δ (ppm): 55.01, 53.46, 18.28, -9.65.

Elemental analysis calculated for $C_{17}H_{39}N_3Ni$: C, 59.32, H 11.42, N 12.21. Found: C 59.36, H 11.47, N 12.27.

The full characterization of this complex will be reported separately.[4]

Synthesis of [(iPr$_3$TACN)Ni^{II}NO]PF$_6$

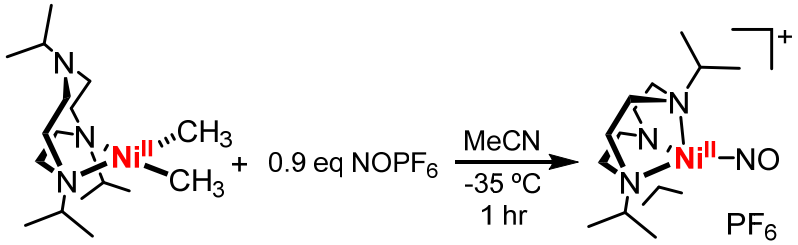

(iPr$_3$TACN)NiMe$_2$ (37 mg, 0.11 mmol) was dissolved in 4 mL of MeCN and cooled to -35 ºC. The NOPF$_6$ (16.9 mg, 0.09 mmol, 0.9 equiv) dissolved in 0.5 mL of cold MeCN and added dropwise to the cold stirring solution as the color quickly changed to dark violet. The reaction was stirred for 30 min at RT and then filtered through a small Celite column to collect a clear violet filtrate. The solution was concentrated to 2 mL and the product was precipitated after the addition of Et$_2$O (5 mL). The light violet powder was collected, rinsed with Et$_2$O, and dried under vacuum. Crystals suitable for X-ray crystallography were grown using through vapor diffusion of Et$_2$O in a concentrated solution of MeCN at -35 ºC. Yield: 33 mg, 63%. The procedure can also be done using NOBF$_4$ as the oxidant.

NMR: ^{1}H NMR (499 MHz, CD$_3$CN) δ 4.28 (s, 3H), 3.34 (s, 7H), 2.18 (s, 9H), 1.62 (s, 19H).
ESI-MS (*m*/*z*): Calc 343.2001, Found 343.2008
Elemental analysis calculated for C$_{15}$H$_{33}$N$_4$NiOPF$_6$•0.1Et$_2$O: C, 37.25; H, 6.90; N, 11.28. Found: C, 37.35; H, 7.28; N, 10.88.

Note 1: The C–C bond formation product was observed by monitoring the reaction via NMR. Analysis of the *in-situ* reaction led to the observation of ethane in 66 % yield after 1 hour at room temperature.

Note 2: The reaction with 1-1.1 equiv NOPF$_6$ resulted in the formation of a mixture of [(iPr$_3$TACN)Ni^{II}NO]PF$_6$ and a second species identified by single crystal X-ray diffraction as [(iPr$_3$TACN)Ni^{II}(NOCH$_3$ON]PF$_6$. The structural parameters for the latter species can be found in Tables S5–S7 and Figure S16.

Synthesis of $[(iPr_3TACN)Ni^{II}(MeCN)_2](PF_6)_2$

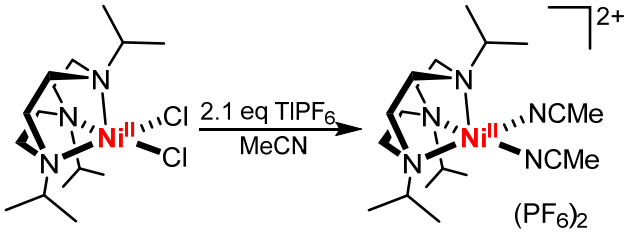

$[(iPr_3TACN)Ni^{II}(MeCN)_2](PF_6)_2$: $(iPr_3TACN)NiCl_2$ (300 mg, 0.78 mmol) was dissolved/suspended in 10 mL of MeCN. 2.1 eq of $TlPF_6$ (572 mg, 1.6 mmol) was then added as a white solid to the stirring yellow/green solution. A dark blue color quickly formed along with a white precipitate and allowed to stir for overnight. The solution was filtered through a small Celite column to collect a clear blue filtrate, which was then concentrated to 2 mL. Et_2O (5-7 mL) was then layered on the solution and set to crystallize overnight. Blue crystalline material was collected, washed with a minimum amount of cold MeCN:Et_2O (1:1) followed by an Et_2O rinse and dried under vacuum. Crystals suitable for X-ray crystallography were grown from vapor diffusion of Et_2O into a concentrated MeCN solution of the complex. Yield: 501 mg, 94%.

NMR: ^{1}H-NMR (500 MHz, CD_3CN), δ (ppm): 8.04 (br)

ESI-MS: The formate adduct was observed $[(iPr_3TACN)Ni^{II}(HCOO)]^+$ at 358.1999 g/mol.

Elemental analysis calculated for $C_{15}H_{33}N_3NiP_2F_{12}(MeCN)_2$: C, 33.26, H 5.73, N 10.21. Found: C 33.82, H 5.71, N 10.57.

Evans method (MeCN): $\mu_{eff} = 2.86\ \mu_B$

Synthesis of [(iPr$_3$TACN)Ni^{II}(CN^{t}Bu)$_3$](PF$_6$)$_2$

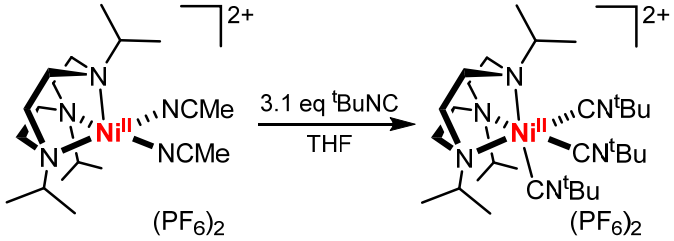

Method A: [(iPr$_3$TACN)Ni^{II}(MeCN)$_2$](PF$_6$)$_2$ (100 mg, 0.15 mmol) was dissolved in 5 mL of MeCN. Tert-butyl isocyanide (^{t}BuNC) (52.8 µL, 0.47 mmol) was then added to the stirring solution as a colorless liquid as the color quickly changed to a brown/red color. Et$_2$O (5 mL) was then added to the solution to precipitate a light green powder. The powder was collected, rinsed with Et$_2$O (3 x 2 mL) and dried under vacuum. Crystals suitable for X-ray crystallography were grown from a vapor diffusion of Et$_2$O into concentrated MeCN reaction done with the addition of 2 eq of ^{t}BuNC. Yield: 97 mg, 78%

Method B: [(iPr$_3$TACN)Ni^{II}(MeCN)$_2$](PF$_6$)$_2$ (200 mg, 0.15 mmol) blue crystals were suspended in 4 mL of THF. Tert-butyl isocyanide (^{t}BuNC) (102 µL, 0.47 mmol) was then added to the stirring solution as a colorless liquid and left to stir for 16 hours at RT. A pale green powder formed, collected, rinsed with Et$_2$O (3 x 2 mL) and dried under vacuum. Yield: 234 mg, 94%

Elemental analysis calculated for C$_{15}$H$_{33}$N$_3$NiP$_2$F$_{12}$·(^{t}BuNC)$_3$: C, 42.22, H 7.09, N 9.85. Found: C 42.27, H 6.82, N 9.67.

Evans method (MeCN): μ_{eff} = 2.60 μ_B

Synthesis of $[(iPr_3TACN)Ni^{I}(CN^{t}Bu)_2]PF_6$

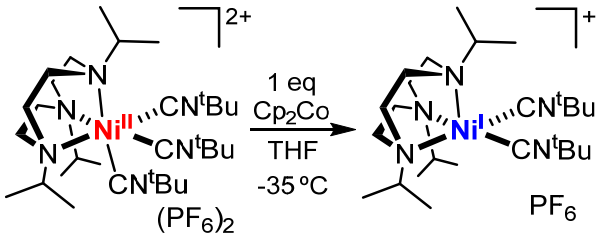

Method A: $[(iPr_3TACN)Ni^{II}(MeCN)_2](PF_6)_2$ (50 mg, 0.07 mmol) was dissolved in 5 mL of MeCN. A separate solution was prepared for Cp_2Co (13.8 mg, 0.07 mmol) in MeCN. Both solutions were cooled to -35 ºC and the reductant added dropwise as the color quickly changed to a yellow-green color. Et_2O (5 mL) was then added to the solution to precipitate cobaltocenium as a green/yellow powder and a yellow-green solution. The filtrate was concentrated to 1 mL and precipitated to collect a brown/yellow powder. The powder was collected and dried under vacuum. Green/yellow crystals suitable for X-ray crystallography were grown from a vapor diffusion of Et_2O into concentrated MeCN. Yield: 36 mg, 79 %

Note: Et_2O to precipitate the product must be added slowly to prevent simultaneous precipitation of $[Cp_2Co]PF_6$, an orange solid.

Method B: $[(iPr_3TACN)Ni^{II}(MeCN)_2](PF_6)_2$ (50 mg, 0.07 mmol) was suspended in 1-2 mL of THF. A separate solution was prepared for Cp_2Co (13.8 mg, 0.07mmol) in THF. Both solutions were cooled to -35 ºC and the reductant added dropwise. The color quickly changed to a yellow-green color as cobaltocenium precipitated as a yellow/green powder. The solution was filtered through collect a clear yellow-green filtrate. Et_2O (5 mL) was then added to the solution to precipitate a brown/yellow powder. The powder was collected and dried under vacuum. Yield: 40 mg, 88 %

Note: Method B worked well to easily remove the cobaltocenium byproduct as it is insoluble in THF.

Elemental analysis calculated for $C_{15}H_{33}N_3NiPF_6(^{t}BuNC)_2$: C, 48.02; H, 8.22; N, 11.20. Found: C, 48.31; H, 8.25; N, 11.11.

Evans method (MeCN): $\mu_{eff} = 1.68\ \mu_B$

III. NMR Spectra

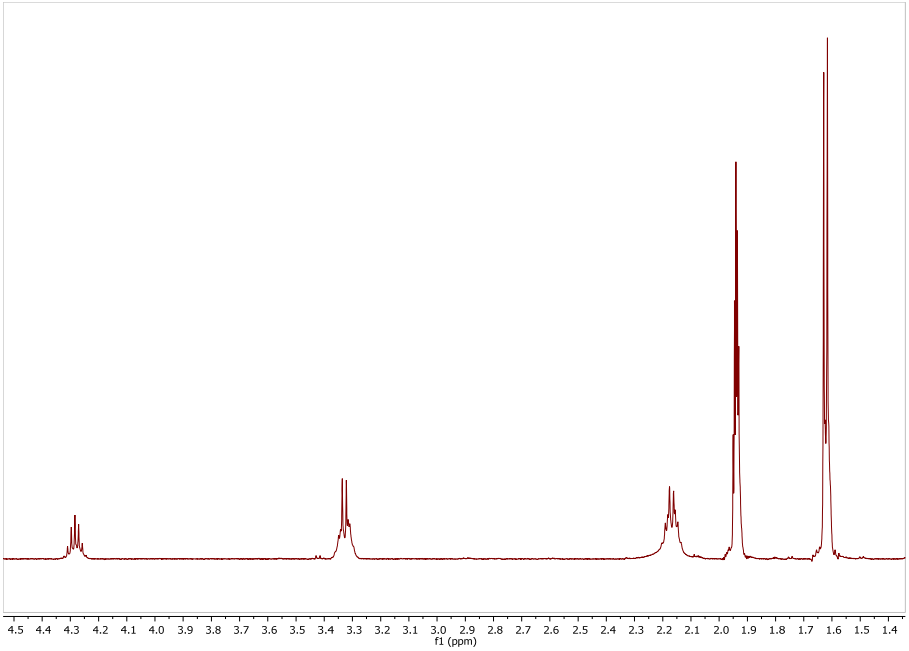

Figure S1. ^{1}H NMR for [(iPr$_3$TACN)Ni^{II}NO]PF$_6$, **2**, (500 MHz, CD$_3$CN) δ 4.29 (hept, *J* = 6.5 Hz, 3H), 3.38 – 3.26 (m, 6H), 2.25 – 2.10 (m, 6H), 1.62 (d, *J* = 6.7 Hz, 18H).

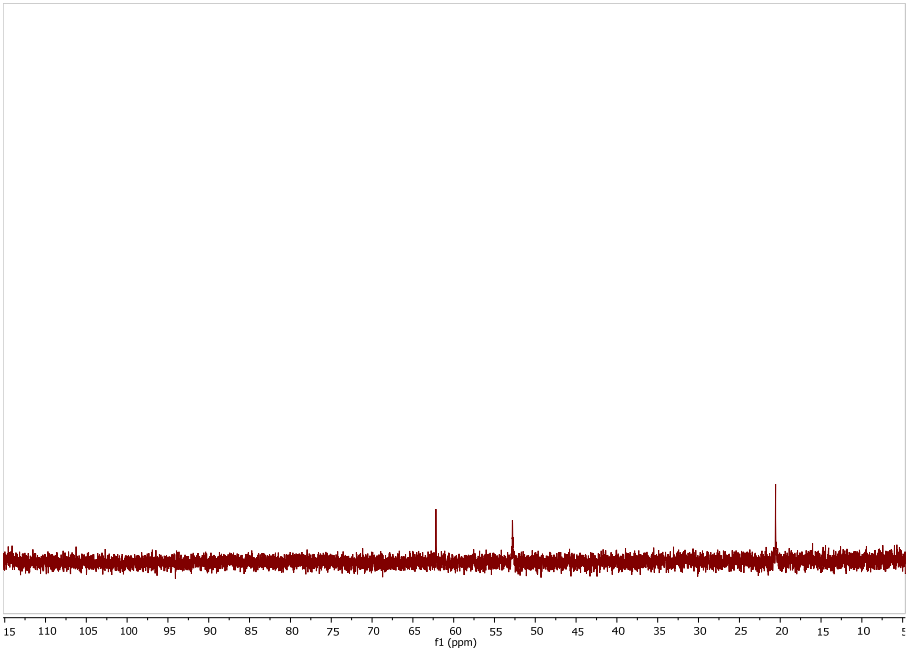

Figure S2. ^{13}C NMR for [(iPr$_3$TACN)Ni^{II}NO]PF$_6$, **2**, (500 MHz, CD$_3$CN) δ 20.57, 52.80, 62.17

IV. IR Spectra

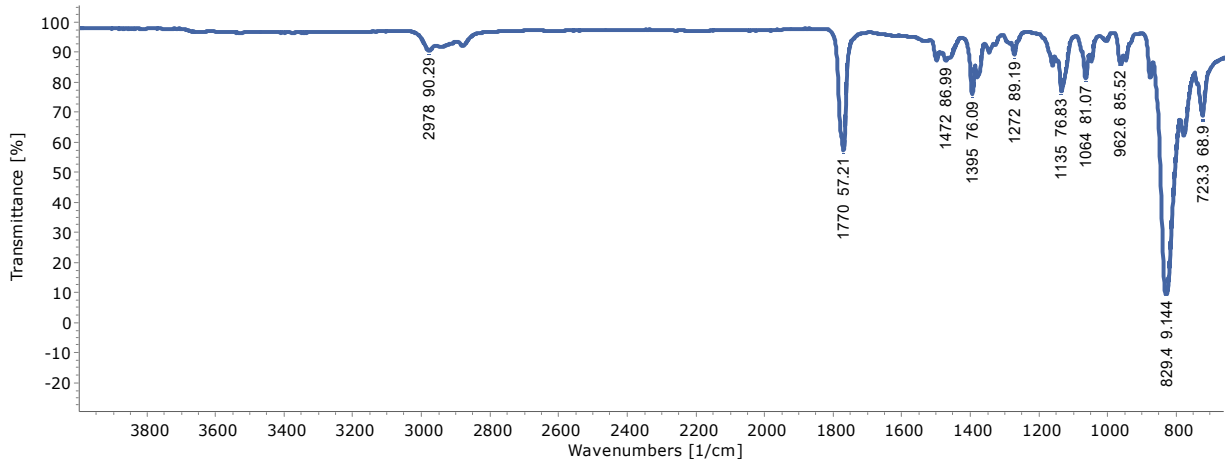

Figure S3. IR spectrum of $[(iPr_3TACN)Ni^{II}NO]PF_6$. IR ($cm^{-1}$): 723 (m), 829 (s), 962 (m), 1064 (m), 1135 (m), 1272 (m), 1395 (m), 1472 (m), 1770 (m), 2978 (m)

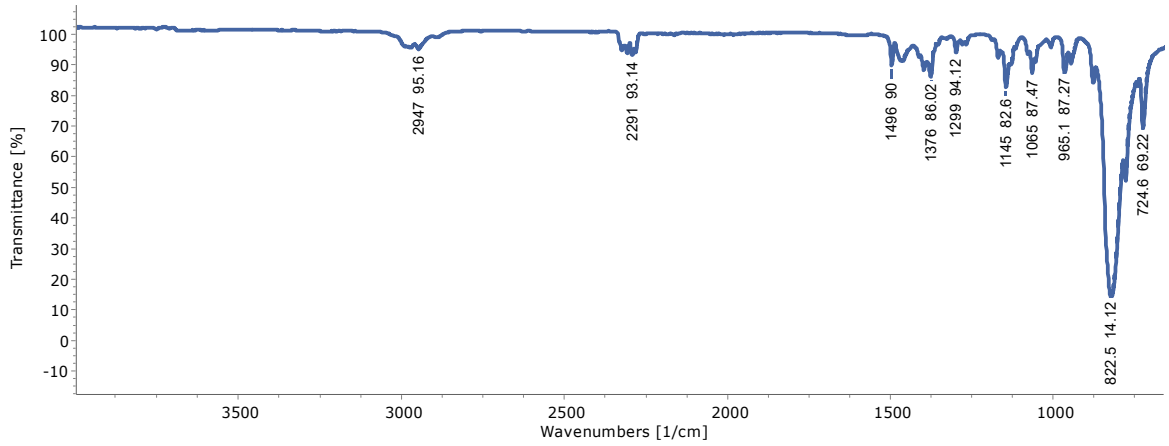

Figure S4. IR spectrum of $[(iPr_3TACN)Ni^{II}(MeCN)_2](PF_6)_2$. IR ($cm^{-1}$): 383 (m), 557 (s), 723 (m), 832 (s), 965 (m), 1065 (m), 1155 (m), 1299 (m), 1375 (m), 1496 (m), 2291 (m), 2947 (m).

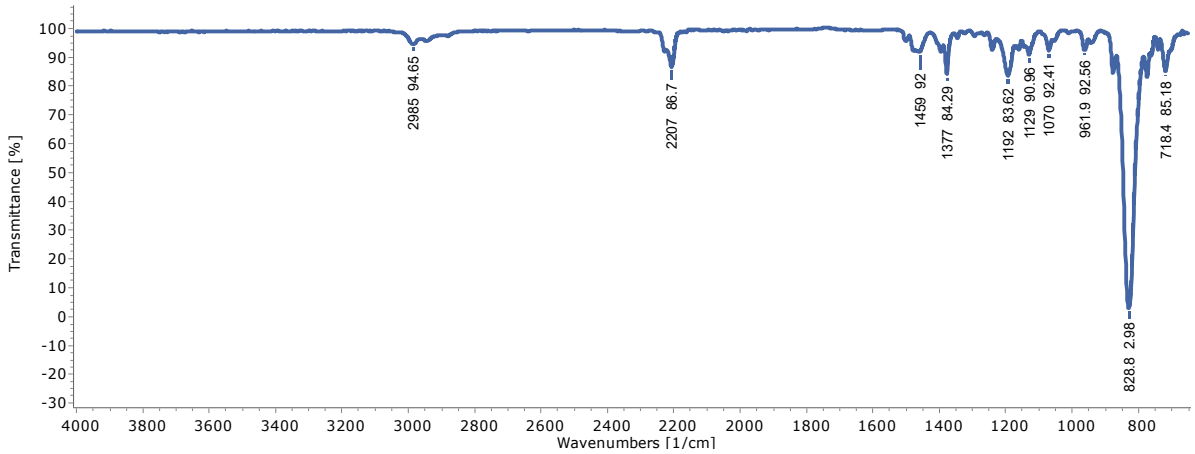

Figure S5. IR spectrum of [(iPr$_3$TACN)Ni^{II}(CN^{t}Bu)$_3$](PF$_6$) from bulk THF reaction. IR (cm^{-1}): 718 (m), 829 (s), 962 (m), 1070 (m), 1129 (m), 1192 (m), 1377 (m), 1459 (m), 2207 (m), 2232 (sh), 2985 (m).

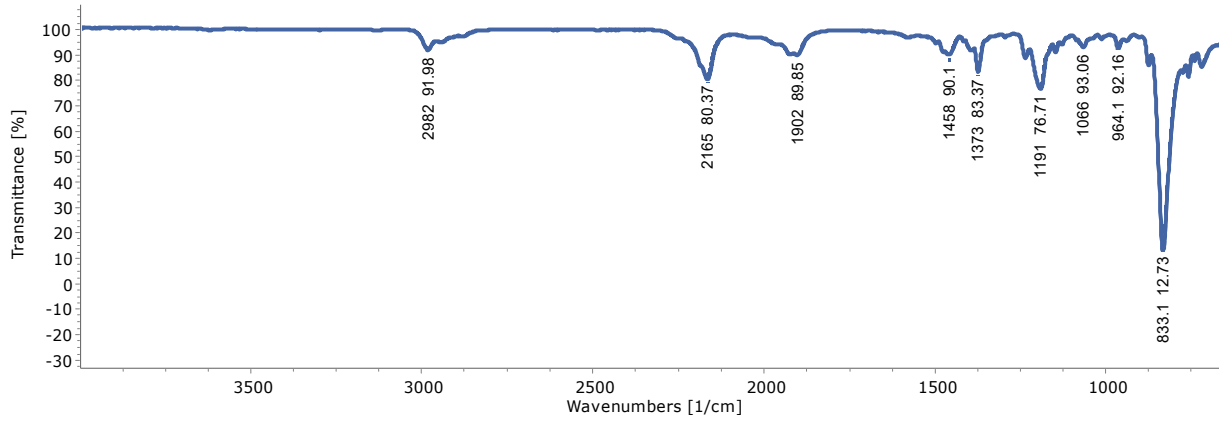

Figure S6. IR spectrum of [(iPr$_3$TACN)Ni^{I}(CN^{t}Bu)$_2$](PF$_6$). IR (cm^{-1}): 833 (s), 964 (m), 1066 (m), 1192 (m), 1373 (m), 1458 (m), 1902 (m), 2165 (m), 2185 (sh), 2982 (m).

IV. Cyclic Voltammetry Experiments

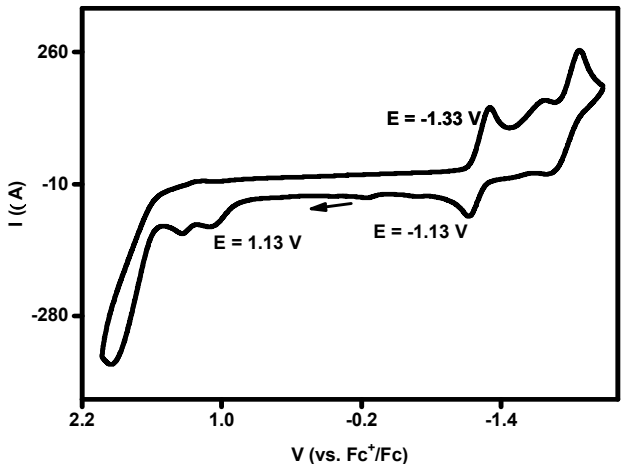

Figure S7. CV of $[(iPr_3TACN)Ni^{II}(MeCN)_2](PF_6)_2$ in 0.1 M *n*-Bu_4NPF_6/MeCN (100 mV/s scan rate). The Ni^{II}/Ni^{I} reduction potential was observed at $E_{1/2}$ = -1.23 V.

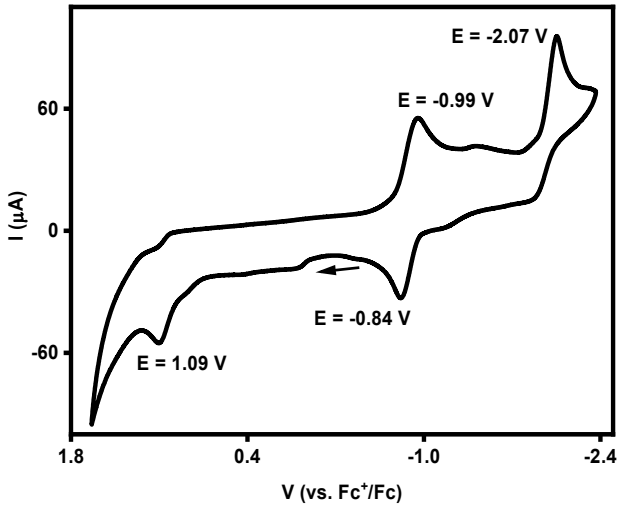

Figure S8. CV of $[(iPr_3TACN)Ni^{II}(CN^tBu)_3](PF_6)_2$ in 0.1 M *n*-Bu_4NPF_6/MeCN (100 mV/s scan rate). The Ni^{II}/Ni^{I} reduction potential was observed at $E_{1/2}$ = -0.92 V.

V. UV-Vis Spectra

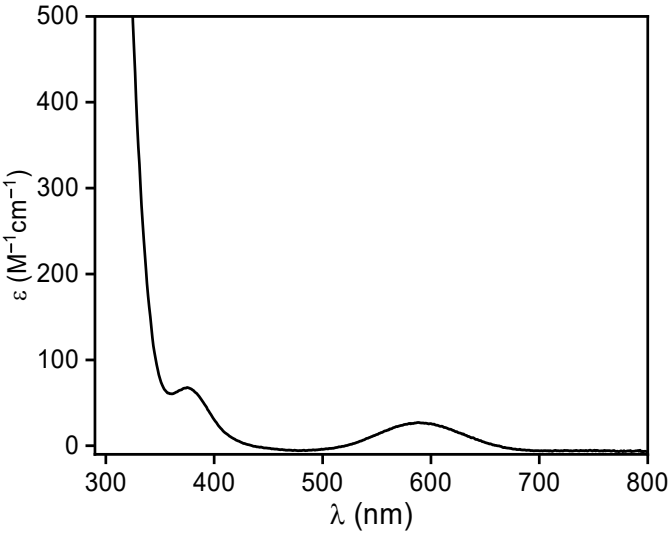

Figure S9. UV-vis absorption spectrum of $[(iPr_3TACN)Ni^{II}(MeCN)_2](PF_6)_2$ (3.5 mM in MeCN).

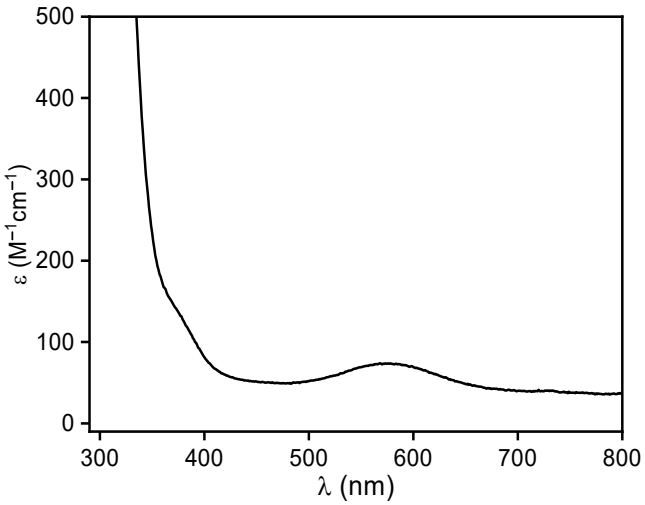

Figure S10. UV-vis absorption spectrum of $[(iPr_3TACN)Ni^{II}(CN^tBu)_3](PF_6)_2$ (2.3 mM in MeCN).

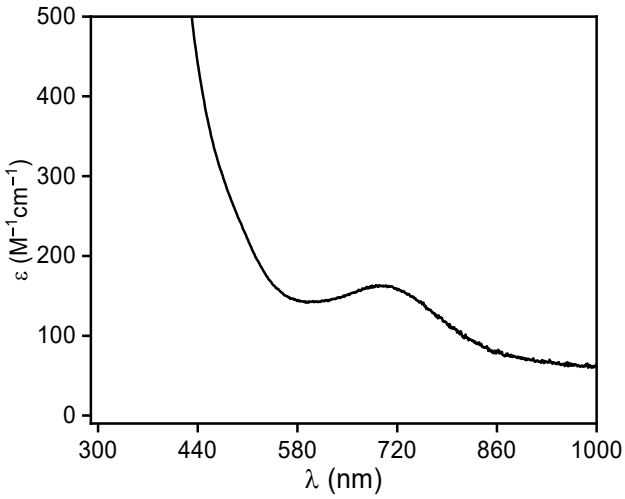

Figure S11. UV-vis absorption spectrum of [(iPr$_3$TACN)Ni^{I}(CN^{t}Bu)$_2$](PF$_6$) (1.6 mM in MeCN).

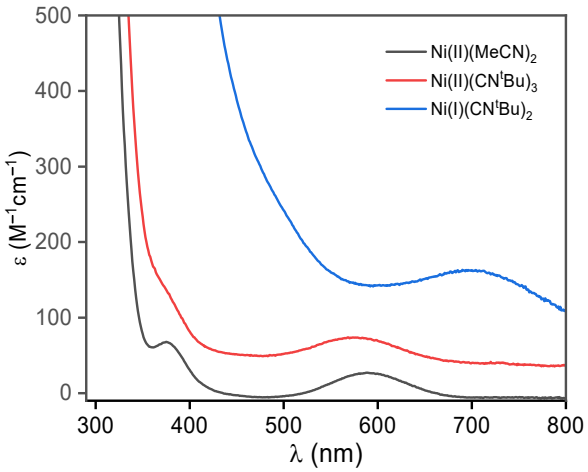

Figure S12. Overlayed UV-vis absorption spectra for [(iPr$_3$TACN)Ni^{II}(MeCN)$_3$](PF$_6$)$_2$ (black), [(iPr$_3$TACN)Ni^{II}(CN^{t}Bu)$_3$](PF$_6$)$_2$ (red), and [(iPr$_3$TACN)Ni^{I}(CN^{t}Bu)$_2$](PF$_6$) (blue) in MeCN.

VI. EPR Spectra and Simulations of Ni^{I} Complex

General procedure preparation and analysis of the Ni^{I}. All sample preparations were conducted in a glovebox with a N_2 atmosphere at -35 ºC. Solvent mixtures containing glassing solvents, butyronitrile (PrCN), or 2-methyltetrahydrofuran (2-MeTHF) were prepared separately with MeCN or THF, respectively, in a 3:1 mixture. An EPR tube was charged with a solution of $[(iPr_3TACN)Ni^{II}(CN^tBu)_3](PF_6)_2$ (4 mg, 4.7 μmmol) or $[(Me_3TACN)Ni^{II}(CN^tBu)_3](PF_6)_2$ (4 mg, 6.1 μmol) in 0.2 mL of solvent mixture. 0.2 mL of the solvent mixture was also used to prepare a solution containing 1 equivalent of reductant or oxidant [cobaltocene (Cp_2Co) or NOPF6,] and added to the complex. The solution mixture (0.4 mL, 11.7-15.3 mM) of 1:3 MeCN:PrCN or 1:3 THF:2-MeTHF was sealed, removed from the glovebox, mixed for 5 seconds, and frozen in liquid nitrogen. Warmup temperatures were done by allowing the solution to thaw at RT.

Experimental conditions: temperature: 77 K, frequency ≈ 9.097 GHz, power = 1 mW, modulation frequency = 100 kHz, modulation amplitude = 3 G, time constant = 0.3 s. Simulation parameters: Gaussian linewidth = 15-40 G.

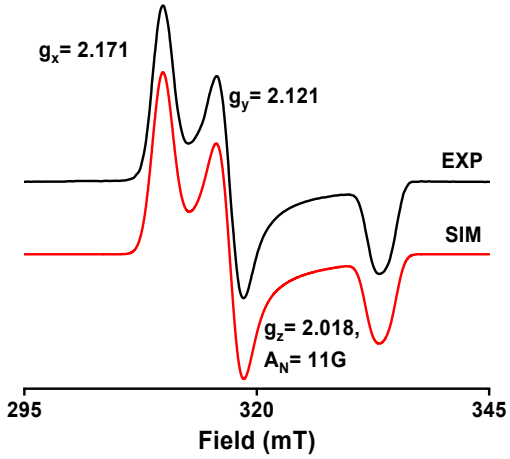

Figure S13. Experimental (MeCN:PrCN (1:3) glass, 77 K) and simulated EPR spectra of $[(iPr_3TACN)Ni^I(CN^tBu)_2]^+$ (**5**) The following parameters were used for simulations: g_x = 2.171; g_y = 2.121; g_z = 2.018 (A_N = 11.0 G).

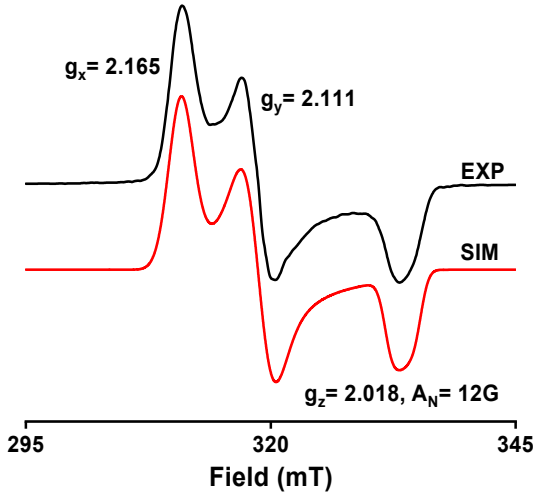

Figure S14. Experimental (THF:2MeTHF (1:3) glass, 77 K) and simulated EPR spectra of $[(Me_3TACN)Ni^I(CN^tBu)_2]^+$. The following parameters were used for simulations: g_x = 2.165; g_y = 2.111; g_z = 2.018 (A_N = 12.0 G).

Table S1. Calculated and simulated g-values and superhyperfine coupling constants (A).

$[(iPr_3TACN)Ni^I(CN^tBu)_2]^+$ (**5**)	g-value			A (G)
Experimental	2.018	2.121	2.171	11.0
Simulation	2.018	2.121	2.171	11.0
Calculated (DFT)	2.044	2.198	2.264	

VIII. DFT Calculations

The density functional theory (DFT) calculations for the complex **5** $[(iPr_3TACN)Ni^{I}(CN^{t}Bu)_2]^{+}$ were performed using software package Gaussian 16.[11] Single point energy, EPR parameters, and TD-DFT calculations were performed using the crystallographic coordinates for **5**. The M06[12] functional along with the tzvp[13-14] basis set were employed, since this combination of hybrid functional and basis set has been previously shown to work well for reproducing experimental parameters for Ni complexes.[15-16] The atomic contributions to frontier molecular orbitals were analyzed using the program Chemissian.[17]

Table S2. Atomic contributions of selected molecular orbitals for $[(iPr_3TACN)Ni^{I}(CN^{t}Bu)_2]PF_6$ (**5**).

MO	MOs (0.07 isocontour value)	Ni	N	C
α-HOMO	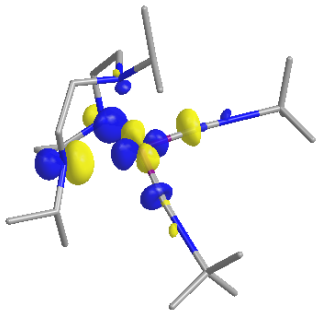	40%	31%	19%
β-HOMO	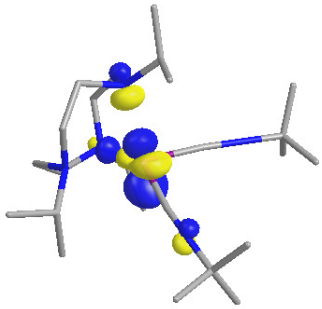	71%	19%	5%

α-LUMO	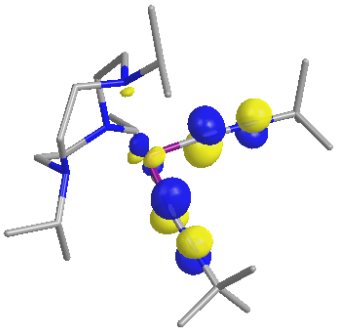	12%	20%	50%
β-LUMO	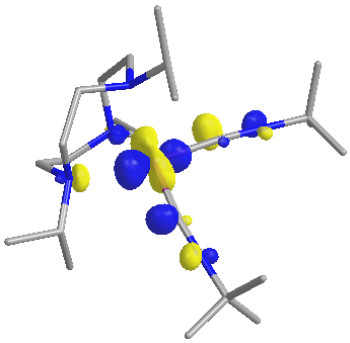	58%	6%	24%

IX. X-ray Structure Determinations of (iPr_3TACN)Ni Complexes

General information.

Single crystals were grown by vapor diffusion of diethyl ether into concentrated solution of acetonitrile at -35 ºC. Crystals were mounted on a Bruker D8 Venture kappa diffractometer equipped with a Photon II CPAD detector. An Iμs microfocus Mo source (λ = 0.71073 Å) coupled with a multi-layer mirror monochromator provided the incident beam. The sample was mounted on a nylon loop with the minimal amount of Paratone-N oil. Data was collected as a series of φ and/or ω scans. Data were collected at 100 K using a cold stream of N_2(g). The collection, cell refinement, and integration of intensity data was carried out with the APEXIII software.[18] A multiscan absorption correction was performed with SADABS or TWINABS-2012/1.[19] The structure was phased with intrinsic methods using SHELXT and refined with the full-matrix least-squares program SHELXL.[20] Hydrogen atoms were placed in calculated positions using the standard riding model and refined isotropically; all non-hydrogen atoms were refined anisotropically.

Software and solutions: SAINT V8.38A, SHELXT, XL, Olex2.[20-22]

The deposition numbers 2167418 (**2**) 2166722 (**3**)**,** 2166723 (**4**)**,** 2166724 (**5**) and 2167752 (**[(iPr_3TACN)$Ni^{II}(ONCH_3NO)_2$]PF_6**) at the Cambridge Crystallographic Data Centre (CCDC) contain the supplementary crystallographic data. This data is provided free of charge by the Cambridge Crystallographic Data Centre. Crystallographic details are summarized in Tables S2–S16.

[(iPr$_3$TACN)Ni^{II}NO]BF$_4$ (2)

Table S3. Crystal data and structure refinement for [(iPr$_3$TACN)Ni^{II}NO]BF$_4$.

Identification code	[iPrTACNNiNO]BF4
Empirical formula	$C_{15}H_{33}BF_4N_4NiO$
Formula weight	430.97
Temperature/K	99.99
Crystal system	trigonal
Space group	R3c
a/Å	22.2530(4)
b/Å	22.2530(4)
c/Å	27.3228(5)
α/°	90
β/°	90
γ/°	120
Volume/Å^3	11717.4(5)
Z	23.99994
ρ_{calc}g/cm^3	1.466
μ/mm^{-1}	1.042
F(000)	5472.0
Crystal size/mm^3	0.425 × 0.254 × 0.176
Radiation	MoKα (λ = 0.71073)
2Θ range for data collection/°	5.174 to 56.622
Index ranges	-29 ≤ h ≤ 29, -29 ≤ k ≤ 29, -36 ≤ l ≤ 36
Reflections collected	72926
Independent reflections	6490 [R_{int} = 0.0367, R_{sigma} = 0.0164]
Data/restraints/parameters	6490/188/367
Goodness-of-fit on F^2	1.032
Final R indexes [I>=2σ (I)]	R_1 = 0.0216, wR_2 = 0.0532
Final R indexes [all data]	R_1 = 0.0232, wR_2 = 0.0544
Largest diff. peak/hole / e Å^{-3}	0.35/-0.39
Flack parameter	-0.007(3)

Table S4. Bond Lengths for [(iPr$_3$TACN)Ni^{II}NO]BF$_4$.

Atom	Atom	Length/Å	Atom	Atom	Length/Å
Ni1	N1	2.042(2)	N5	C10	1.501(3)
Ni1	N1^1	2.042(2)	N5	C18	1.508(3)
Ni1	N1^2	2.042(2)	C6	C7	1.520(3)
Ni1	N2	1.677(4)	C8	C9	1.521(3)
O1	N2	1.123(5)	C10	C11	1.523(3)
N1	C1	1.487(3)	C12	C13	1.523(4)
N1	C2	1.496(3)	C12	C14	1.529(4)
N1	C3	1.505(3)	C15	C16	1.521(3)

C1	C2[1]	1.523(4)	C15	C17	1.527(4)
C2	C1[2]	1.523(4)	C18	C19	1.521(3)
C3	C4	1.522(4)	C18	C20	1.532(3)
C3	C5	1.527(3)	F1	B1	1.364(10)
Ni2	N3	2.0481(19)	F2	B1	1.356(10)
Ni2	N4	2.062(2)	F3	B1	1.372(10)
Ni2	N5	2.0467(19)	F4	B1	1.355(10)
Ni2	N6	1.646(2)	F5	B2	1.379(6)
O2	N6	1.162(3)	F6	B2	1.389(6)
N3	C6	1.496(3)	F7	B2	1.363(6)
N3	C11	1.490(3)	F8	B2	1.354(6)
N3	C12	1.510(3)	F9	B3	1.371(5)
N4	C7	1.495(3)	F10	B3	1.389(2)
N4	C8	1.505(3)	B3	F10[2]	1.389(2)
N4	C15	1.512(3)	B3	F10[1]	1.389(2)
N5	C9	1.492(3)			

Table S5. Bond Angles for [(iPr_3TACN)Ni^{II}NO]BF_4.

Atom	Atom	Atom	Angle/°	Atom	Atom	Atom	Angle/°
N1[1]	Ni1	N1[2]	87.35(8)	C9	N5	C18	110.72(17)
N1[1]	Ni1	N1	87.35(8)	C10	N5	Ni2	106.85(13)
N1[2]	Ni1	N1	87.35(8)	C10	N5	C18	110.70(17)
N2	Ni1	N1	127.12(6)	C18	N5	Ni2	114.52(13)
N2	Ni1	N1[1]	127.12(6)	O2	N6	Ni2	170.9(2)
N2	Ni1	N1[2]	127.12(6)	N3	C6	C7	111.62(19)
C1	N1	Ni1	103.10(14)	N4	C7	C6	111.60(19)
C1	N1	C2	111.30(19)	N4	C8	C9	111.03(19)
C1	N1	C3	109.85(19)	N5	C9	C8	110.94(18)
C2	N1	Ni1	107.69(15)	N5	C10	C11	112.00(18)
C2	N1	C3	113.01(19)	N3	C11	C10	111.06(18)
C3	N1	Ni1	111.42(14)	N3	C12	C13	112.9(2)
O1	N2	Ni1	180.0	N3	C12	C14	111.5(2)
N1	C1	C2[2]	111.1(2)	C13	C12	C14	111.0(2)
N1	C2	C1[1]	111.15(19)	N4	C15	C16	111.75(19)
N1	C3	C4	111.7(2)	N4	C15	C17	111.18(19)
N1	C3	C5	114.1(2)	C16	C15	C17	109.2(2)
C4	C3	C5	111.0(2)	N5	C18	C19	111.61(18)
N3	Ni2	N4	87.21(8)	N5	C18	C20	111.63(18)
N5	Ni2	N3	87.84(7)	C19	C18	C20	109.6(2)
N5	Ni2	N4	86.77(7)	F1	B1	F3	108.3(13)
N6	Ni2	N3	120.88(9)	F2	B1	F1	112.0(13)

N6	Ni2	N4	134.72(9)	F2	B1	F3	107.6(10)
N6	Ni2	N5	125.42(9)	F4	B1	F1	111.3(13)
C6	N3	Ni2	107.91(14)	F4	B1	F2	109.3(11)
C6	N3	C12	113.56(19)	F4	B1	F3	108.1(10)
C11	N3	Ni2	102.77(13)	F5	B2	F6	108.7(6)
C11	N3	C6	111.51(19)	F7	B2	F5	110.9(6)
C11	N3	C12	109.8(2)	F7	B2	F6	106.8(4)
C12	N3	Ni2	110.72(16)	F8	B2	F5	110.4(6)
C7	N4	Ni2	102.63(14)	F8	B2	F6	106.1(5)
C7	N4	C8	109.69(18)	F8	B2	F7	113.6(6)
C7	N4	C15	110.35(18)	F9	B3	$F10^{1}$	109.1(2)
C8	N4	Ni2	107.75(14)	F9	B3	$F10^{2}$	109.1(2)
C8	N4	C15	109.72(17)	F9	B3	F10	109.1(2)
C15	N4	Ni2	116.40(14)	$F10^{1}$	B3	F10	109.8(2)
C9	N5	Ni2	104.39(13)	$F10^{2}$	B3	F10	109.8(2)
C9	N5	C10	109.36(18)	$F10^{1}$	B3	$F10^{2}$	109.8(2)

Figure S15. Projection view with 50% probability ellipsoids:

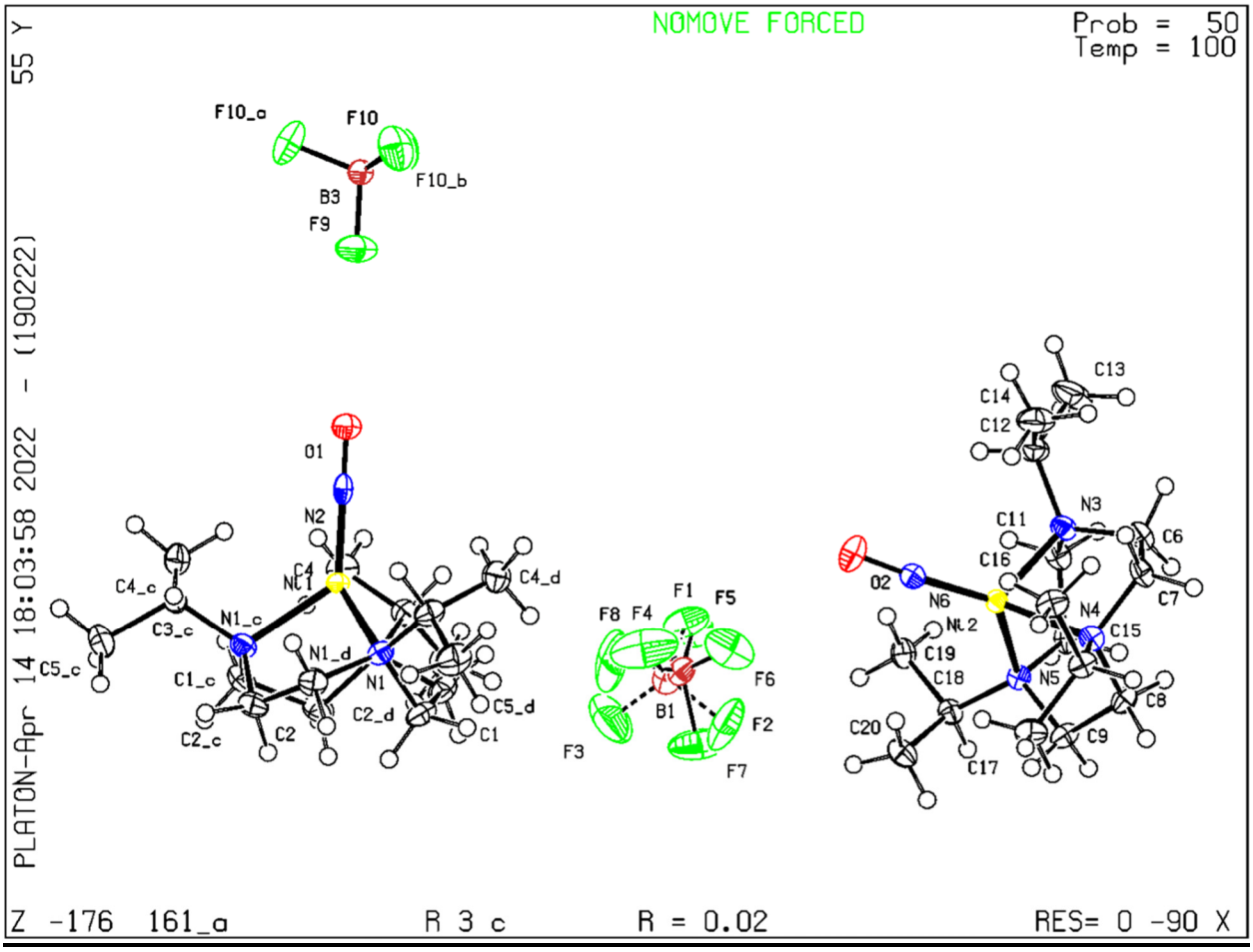

[(iPr$_3$TACN)Ni^{II}(ONCH$_3$NO)$_2$]PF$_6$

Table S6. Crystal data and structure refinement for [(iPr$_3$TACN)Ni^{II}(ONCH$_3$NO)$_2$]PF$_6$.

Identification code	[iPrTACNNiONCH3NO]PF6
Empirical formula	$C_{18}H_{39}F_6N_6NiO_2P$
Formula weight	575.23
Temperature/K	100.0
Crystal system	monoclinic
Space group	$P2_1/c$
a/Å	8.4457(2)
b/Å	14.5310(4)
c/Å	20.9391(6)
α/°	90
β/°	93.8700(10)
γ/°	90
Volume/Å^3	2563.88(12)
Z	4
ρ_{calc}g/cm^3	1.490
μ/mm^{-1}	0.890
F(000)	1208.0
Crystal size/mm^3	0.29 × 0.167 × 0.054
Radiation	MoKα (λ = 0.71073)
2Θ range for data collection/°	4.802 to 56.602
Index ranges	$-11 \le h \le 11$, $-19 \le k \le 19$, $-27 \le l \le 27$
Reflections collected	47944
Independent reflections	6379 [R_{int} = 0.0393, R_{sigma} = 0.0222]
Data/restraints/parameters	6379/0/315
Goodness-of-fit on F^2	1.025
Final R indexes [I>=2σ (I)]	R_1 = 0.0351, wR_2 = 0.0848
Final R indexes [all data]	R_1 = 0.0408, wR_2 = 0.0882
Largest diff. peak/hole / e Å^{-3}	1.04/-0.48

Table S7. Bond Lengths for [(iPr$_3$TACN)Ni^{II}(ONCH$_3$NO)$_2$]PF$_6$.

Atom	Atom	Length/Å	Atom	Atom	Length/Å
Ni1	O1	1.9680(12)	N4	N5	1.276(2)
Ni1	N1	2.0735(15)	N4	C16	1.461(2)
Ni1	N2	2.0569(14)	C5	C6	1.524(2)
Ni1	O2	2.0024(13)	C7	C8	1.527(3)
Ni1	N3	2.0909(14)	C7	C9	1.522(2)
O1	N5	1.308(2)	C10	C11	1.526(3)
C1	C2	1.526(2)	C10	C12	1.533(3)
C1	N3	1.492(2)	C13	C14	1.529(2)
N1	C2	1.486(2)	C13	C15	1.522(3)

N1	C3	1.500(2)	F1	P1	1.5918(18)
N1	C10	1.508(2)	P1	F2	1.5938(15)
N2	C4	1.494(2)	P1	F3	1.5994(17)
N2	C5	1.496(2)	P1	F4	1.5895(14)
N2	C13	1.509(2)	P1	F5	1.5790(16)
O2	N4	1.3212(19)	P1	F6	1.5855(15)
N3	C6	1.489(2)	N6	C17	1.107(4)
N3	C7	1.516(2)	C17	C18	1.417(5)
C3	C4	1.516(3)			

Table S8. Bond Angles for [(iPr_3TACN)Ni^{II}($ONCH_3NO)_2$]PF_6.

Atom	Atom	Atom	Angle/°	Atom	Atom	Atom	Angle/°
O1	Ni1	N1	153.26(6)	O2	N4	C16	117.07(15)
O1	Ni1	N2	118.63(6)	N5	N4	O2	123.84(15)
O1	Ni1	O2	78.86(5)	N5	N4	C16	119.10(16)
O1	Ni1	N3	96.24(5)	N2	C4	C3	111.94(15)
N1	Ni1	N3	85.65(6)	N4	N5	O1	112.85(14)
N2	Ni1	N1	88.08(6)	N2	C5	C6	111.63(13)
N2	Ni1	N3	87.23(6)	N3	C6	C5	111.87(14)
O2	Ni1	N1	98.62(6)	N3	C7	C8	113.71(14)
O2	Ni1	N2	95.30(6)	N3	C7	C9	111.01(14)
O2	Ni1	N3	175.09(5)	C9	C7	C8	110.53(15)
N5	O1	Ni1	115.67(11)	N1	C10	C11	111.73(16)
N3	C1	C2	112.29(14)	N1	C10	C12	113.13(16)
C2	N1	Ni1	105.12(11)	C11	C10	C12	109.96(17)
C2	N1	C3	110.60(14)	N2	C13	C14	113.39(15)
C2	N1	C10	111.94(14)	N2	C13	C15	111.25(15)
C3	N1	Ni1	105.83(11)	C15	C13	C14	110.67(15)
C3	N1	C10	110.80(14)	F1	P1	F2	90.64(9)
C10	N1	Ni1	112.26(11)	F1	P1	F3	178.41(12)
C4	N2	Ni1	100.88(10)	F2	P1	F3	89.50(9)
C4	N2	C5	111.94(14)	F4	P1	F1	88.84(9)
C4	N2	C13	109.70(14)	F4	P1	F2	179.36(10)
C5	N2	Ni1	107.47(10)	F4	P1	F3	91.01(9)
C5	N2	C13	112.90(14)	F5	P1	F1	90.25(15)
C13	N2	Ni1	113.35(10)	F5	P1	F2	89.77(10)
N4	O2	Ni1	108.41(10)	F5	P1	F3	91.34(14)
N1	C2	C1	111.08(15)	F5	P1	F4	90.60(10)
C1	N3	Ni1	108.08(10)	F5	P1	F6	179.65(15)
C1	N3	C7	112.95(14)	F6	P1	F1	90.02(11)
C6	N3	Ni1	101.58(10)	F6	P1	F2	90.47(9)

C6	N3	C1	111.37(13)	F6	P1	F3	88.40(9)
C6	N3	C7	109.60(13)	F6	P1	F4	89.17(8)
C7	N3	Ni1	112.71(10)	N6	C17	C18	179.6(6)
N1	C3	C4	111.80(14)				

Figure S16. Projection view with 50% probability ellipsoids:

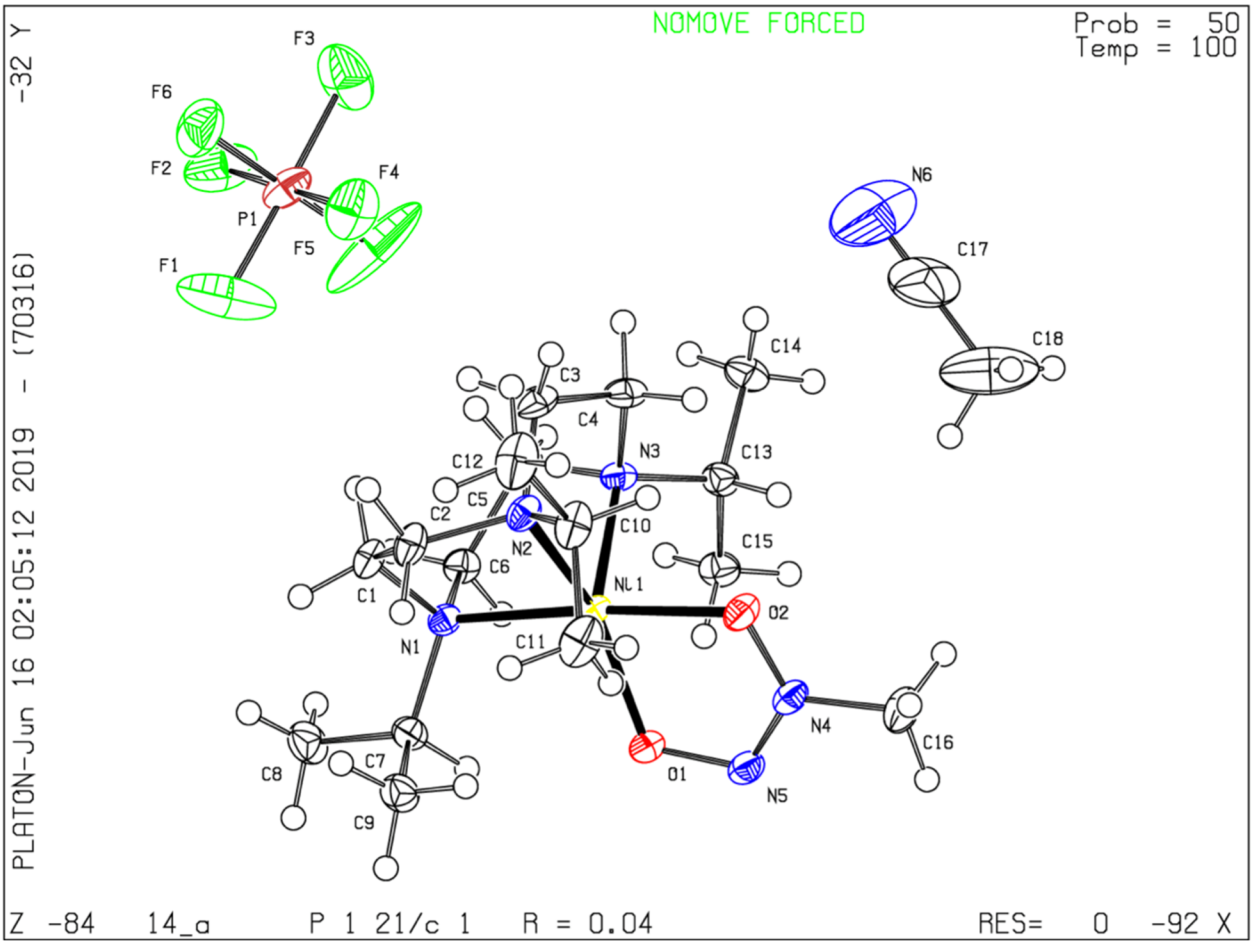

[(iPr$_3$TACN)Ni^{II}(MeCN)$_2$](BF$_4$)$_2$ (3)

Table S9. Crystal data and structure refinement for [(iPr$_3$TACN)Ni^{II}(MeCN)$_2$](BF$_4$)$_2$.

Identification code	[iPrTACNNi(MeCN)2](BF4)2
Empirical formula	$C_{21}H_{42}B_2F_8N_6Ni$
Formula weight	610.93
Temperature/K	100.15
Crystal system	triclinic
Space group	P-1
a/Å	9.9809(3)
b/Å	10.6534(4)
c/Å	14.0509(5)
α/°	86.114(2)
β/°	75.996(2)
γ/°	81.687(2)
Volume/Å^3	1433.57(9)
Z	2
ρ_{calc}g/cm^3	1.415
μ/mm^{-1}	0.751
F(000)	640.0
Crystal size/mm^3	0.657 × 0.372 × 0.104
Radiation	MoKα (λ = 0.71073)
2Θ range for data collection/°	4.58 to 56.612
Index ranges	-13 ≤ h ≤ 13, -14 ≤ k ≤ 14, -18 ≤ l ≤ 18
Reflections collected	35173
Independent reflections	7125 [R_{int} = 0.0329, R_{sigma} = 0.0233]
Data/restraints/parameters	7125/0/352
Goodness-of-fit on F^2	1.056
Final R indexes [I>=2σ (I)]	R_1 = 0.0268, wR_2 = 0.0658
Final R indexes [all data]	R_1 = 0.0301, wR_2 = 0.0678
Largest diff. peak/hole / e Å^{-3}	0.58/-0.40

Table S10. Bond Lengths for [(iPr$_3$TACN)Ni^{II}(MeCN)$_2$](BF$_4$)$_2$

Atom	Atom	Length/Å	Atom	Atom	Length/Å
B1	F1	1.3739(18)	C7	N1	1.5142(14)
B1	F2	1.3785(18)	C10	C11	1.5299(17)
B1	F3	1.3920(18)	C10	C12	1.5211(17)
B1	F4	1.3971(16)	C10	N2	1.5081(14)
B2	F5	1.3923(18)	C13	C14	1.5270(17)
B2	F6	1.3841(17)	C13	C15	1.5254(17)
B2	F7	1.3855(18)	C13	N3	1.5109(15)
B2	F8	1.3718(18)	C16	C17	1.4526(17)

C1	C2	1.5239(15)	C16	N4	1.1355(16)
C1	N1	1.4991(14)	C18	C19	1.4513(17)
C2	N2	1.4893(14)	C18	N5	1.1345(16)
C3	C4	1.5256(16)	N1	Ni1	2.0568(9)
C3	N2	1.4987(14)	N2	Ni1	2.0864(10)
C4	N3	1.4934(14)	N3	Ni1	2.0730(10)
C5	C6	1.5220(15)	N4	Ni1	2.0574(10)
C5	N3	1.4957(14)	N5	Ni1	2.0434(10)
C6	N1	1.4931(14)	C20	C21	1.456(2)
C7	C8	1.5298(16)	C20	N6	1.139(2)
C7	C9	1.5224(16)			

Table S11. Bond Angles for [(iPr_3TACN)Ni^{II}($MeCN)_2$]($BF_4)_2$.

Atom	Atom	Atom	Angle/°	Atom	Atom	Atom	Angle/°
F1	B1	F2	111.24(12)	C1	N1	Ni1	106.68(6)
F1	B1	F3	110.25(13)	C6	N1	C1	111.70(9)
F1	B1	F4	109.74(13)	C6	N1	C7	108.78(8)
F2	B1	F3	108.97(13)	C6	N1	Ni1	100.79(7)
F2	B1	F4	109.11(12)	C7	N1	Ni1	115.88(7)
F3	B1	F4	107.45(11)	C2	N2	C3	111.12(9)
F6	B2	F5	109.83(12)	C2	N2	C10	109.44(9)
F6	B2	F7	107.70(12)	C2	N2	Ni1	101.13(6)
F7	B2	F5	109.50(12)	C3	N2	C10	112.56(9)
F8	B2	F5	108.77(12)	C3	N2	Ni1	108.52(7)
F8	B2	F6	110.74(13)	C10	N2	Ni1	113.52(7)
F8	B2	F7	110.29(13)	C4	N3	C5	110.45(9)
N1	C1	C2	111.97(9)	C4	N3	C13	112.43(9)
N2	C2	C1	112.07(9)	C4	N3	Ni1	105.36(7)
N2	C3	C4	111.79(9)	C5	N3	C13	111.22(9)
N3	C4	C3	110.85(9)	C5	N3	Ni1	105.45(7)
N3	C5	C6	112.12(9)	C13	N3	Ni1	111.56(7)
N1	C6	C5	111.73(9)	C16	N4	Ni1	168.35(10)
C9	C7	C8	110.70(10)	C18	N5	Ni1	164.07(10)
N1	C7	C8	112.98(9)	N1	Ni1	N2	87.92(4)
N1	C7	C9	111.32(9)	N1	Ni1	N3	88.45(4)
C12	C10	C11	111.06(10)	N1	Ni1	N4	94.46(4)
N2	C10	C11	114.18(10)	N3	Ni1	N2	85.51(4)
N2	C10	C12	110.51(10)	N4	Ni1	N2	177.32(4)
C15	C13	C14	109.36(10)	N4	Ni1	N3	95.77(4)
N3	C13	C14	110.74(10)	N5	Ni1	N1	116.80(4)
N3	C13	C15	114.05(10)	N5	Ni1	N2	94.61(4)

N4	C16	C17	179.85(17)	N5	Ni1	N3	154.75(4)
N5	C18	C19	179.82(17)	N5	Ni1	N4	83.23(4)
C1	N1	C7	112.49(9)	N6	C20	C21	178.90(19)

Figure S17. Projection view with 50% probability ellipsoids:

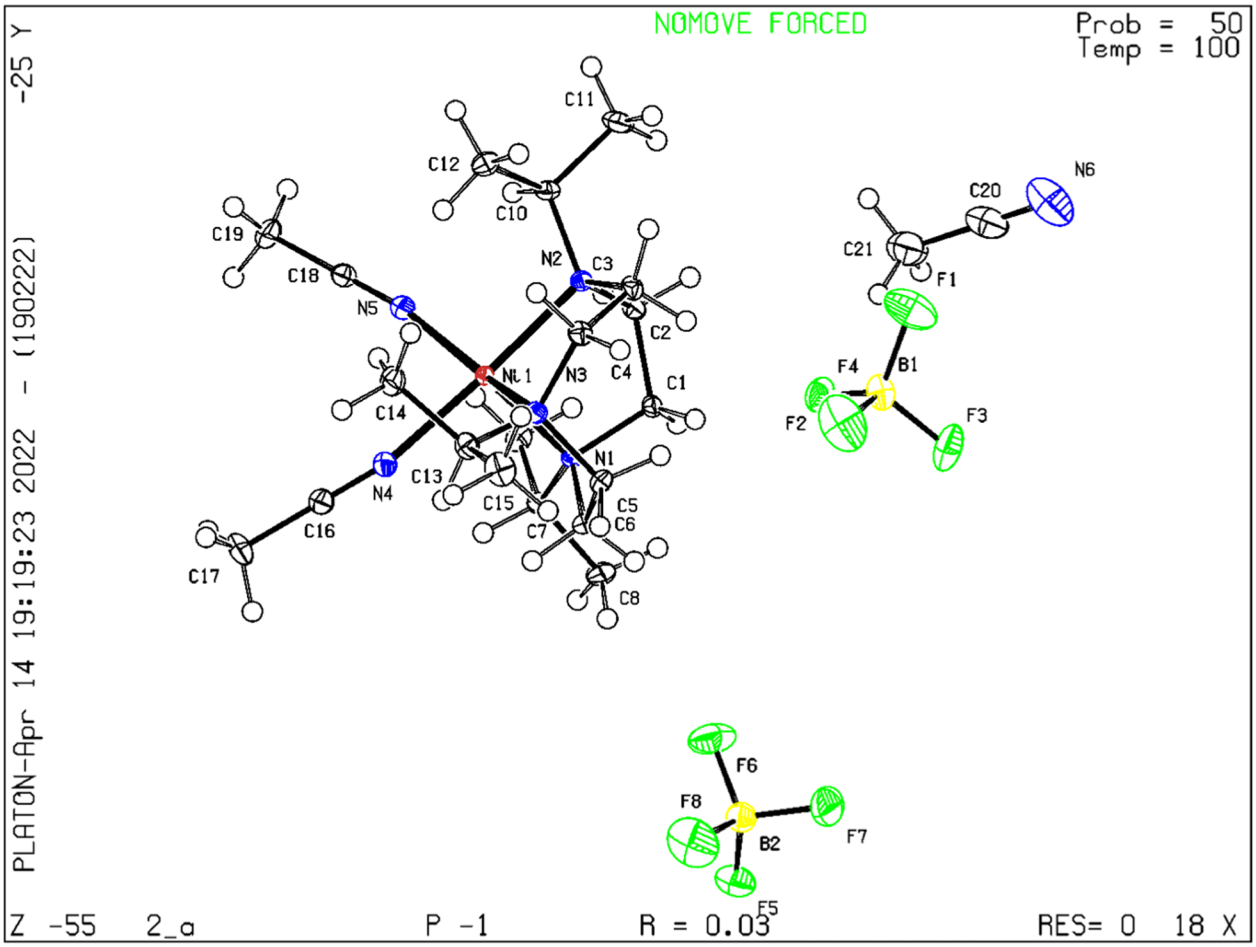

[(iPr$_3$TACN)Ni^{II}(CN^{t}Bu)$_3$](PF$_6$)$_2$ (4)

Table S12. Crystal data and structure refinement for [(iPr$_3$TACN)Ni^{II}(CN^{t}Bu)$_3$](PF$_6$)$_2$.

Identification code	dd62ys
Empirical formula	$C_{30}H_{60}F_{12}N_6NiP_2$
Formula weight	853.49
Temperature/K	100.01
Crystal system	hexagonal
Space group	$P6_3$
a/Å	11.1194(2)
b/Å	11.1194(2)
c/Å	18.1833(3)
α/°	90
β/°	90
γ/°	120
Volume/Å^3	1947.00(8)
Z	1.99998
ρ_{calc}g/cm^3	1.456
μ/mm^{-1}	0.669
F(000)	896.0
Crystal size/mm^3	0.661 × 0.287 × 0.253
Radiation	MoKα (λ = 0.71073)
2Θ range for data collection/°	4.786 to 54.22
Index ranges	-14 ≤ h ≤ 14, -14 ≤ k ≤ 14, -23 ≤ l ≤ 23
Reflections collected	40836
Independent reflections	2884 [R_{int} = 0.0266, R_{sigma} = 0.0111]
Data/restraints/parameters	2884/392/236
Goodness-of-fit on F^2	1.081
Final R indexes [I>=2σ (I)]	R_1 = 0.0622, wR_2 = 0.1723
Final R indexes [all data]	R_1 = 0.0629, wR_2 = 0.1736
Largest diff. peak/hole / e Å^{-3}	1.10/-0.37
Flack parameter	-0.307(13)

Table S13. Bond Lengths for [(iPr$_3$TACN)Ni^{II}(CN^{t}Bu)$_3$](PF$_6$)$_2$.

Atom	Atom	Length/Å	Atom	Atom	Length/Å
Ni1	N1^1	2.125(5)	P2	F3A^4	1.565(12)
Ni1	N1	2.125(5)	P2	F4A^3	1.555(12)
Ni1	N1^2	2.125(5)	P2	F4A	1.555(12)
Ni1	C6^2	1.946(8)	P2	F4A^4	1.555(12)
Ni1	C6	1.946(8)	N1	C1	1.541(10)
Ni1	C6^1	1.946(8)	N1	C2	1.495(9)
P1	F1	1.602(8)	N1	C1A	1.509(13)
P1	F1^2	1.602(8)	N1	C2A	1.524(13)

P1	F1[1]	1.602(8)	N1	C3	1.500(8)
P1	F2[2]	1.603(9)	N2	C6	1.112(12)
P1	F2[1]	1.603(9)	N2	C7	1.467(11)
P1	F2	1.603(9)	C1	C2[2]	1.493(13)
P1	F1A[1]	1.594(13)	C2	C1[1]	1.493(13)
P1	F1A	1.594(13)	C1A	C2A[2]	1.478(16)
P1	F1A[2]	1.594(13)	C2A	C1A[1]	1.478(16)
P1	F2A[1]	1.610(13)	C3	C4	1.526(12)
P1	F2A	1.610(13)	C3	C5	1.542(11)
P1	F2A[2]	1.610(13)	C3	C4A	1.538(15)
P2	F3[3]	1.566(9)	C3	C5A	1.546(15)
P2	F3[4]	1.566(9)	C7	C8	1.502(15)
P2	F3	1.566(9)	C7	C9	1.516(15)
P2	F4[3]	1.557(8)	C7	C10	1.523(15)
P2	F4	1.557(8)	C7	C8A	1.525(16)
P2	F4[4]	1.557(8)	C7	C9A	1.515(16)
P2	F3A	1.565(12)	C7	C10A	1.523(16)
P2	F3A[3]	1.565(12)			

Table S14. Bond Angles for [(iPr$_3$TACN)Ni^{II}(CN^{t}Bu)$_3$](PF$_6$)$_2$.

Atom	Atom	Atom	Angle/°	Atom	Atom	Atom	Angle/°
N1[1]	Ni1	N1	85.9(2)	F4	P2	F3[3]	171.3(8)
N1[2]	Ni1	N1	85.9(2)	F4[3]	P2	F3[4]	171.3(8)
N1[2]	Ni1	N1[1]	85.9(2)	F4[4]	P2	F4[3]	94.6(6)
C6[2]	Ni1	N1[1]	98.9(5)	F4	P2	F4[3]	94.6(6)
C6[1]	Ni1	N1[1]	93.9(4)	F4[4]	P2	F4	94.6(6)
C6[1]	Ni1	N1	98.9(5)	F3A	P2	F3A[4]	92.5(11)
C6[2]	Ni1	N1	175.2(5)	F3A	P2	F3A[3]	92.5(11)
C6	Ni1	N1	93.9(4)	F3A[3]	P2	F3A[4]	92.5(11)
C6[1]	Ni1	N1[2]	175.2(5)	F4A[3]	P2	F3A[3]	92.1(12)
C6	Ni1	N1[1]	175.2(5)	F4A	P2	F3A[3]	173(2)
C6	Ni1	N1[2]	98.9(5)	F4A	P2	F3A	92.1(12)
C6[2]	Ni1	N1[2]	93.9(4)	F4A[3]	P2	F3A	81(2)
C6[1]	Ni1	C6	81.4(4)	F4A[4]	P2	F3A[4]	92.1(12)
C6[2]	Ni1	C6	81.4(4)	F4A[4]	P2	F3A	173(2)
C6[2]	Ni1	C6[1]	81.4(4)	F4A[4]	P2	F3A[3]	81(2)
F1	P1	F1[2]	90.4(5)	F4A	P2	F3A[4]	81(2)
F1	P1	F1[1]	90.4(5)	F4A[3]	P2	F3A[4]	173(2)
F1[2]	P1	F1[1]	90.4(5)	F4A	P2	F4A[3]	94.3(11)
F1	P1	F2[2]	87.6(7)	F4A[4]	P2	F4A	94.3(11)
F1[2]	P1	F2[2]	93.0(8)	F4A[4]	P2	F4A[3]	94.3(11)
F1[2]	P1	F2	176.1(8)	C1	N1	Ni1	98.4(5)

F1	P1	F2	93.0(8)	C2	N1	Ni1	107.9(4)
F1[1]	P1	F2	87.6(7)	C2	N1	C1	110.0(7)
F1	P1	F2[1]	176.1(8)	C2	N1	C3	114.2(7)
F1[2]	P1	F2[1]	87.6(7)	C1A	N1	Ni1	113.2(9)
F1[1]	P1	F2[1]	93.0(8)	C1A	N1	C2A	119.2(15)
F1[1]	P1	F2[2]	176.1(8)	C2A	N1	Ni1	98.3(11)
F2[2]	P1	F2[1]	89.1(7)	C3	N1	Ni1	116.0(5)
F2[2]	P1	F2	89.1(7)	C3	N1	C1	109.2(7)
F2	P1	F2[1]	89.1(7)	C3	N1	C1A	106.4(12)
F1A	P1	F1A[1]	89.8(15)	C3	N1	C2A	103.7(12)
F1A[1]	P1	F1A[2]	89.8(15)	C6	N2	C7	177.2(18)
F1A	P1	F1A[2]	89.8(15)	C2[2]	C1	N1	112.9(8)
F1A[2]	P1	F2A[2]	178(2)	C1[1]	C2	N1	108.5(7)
F1A[1]	P1	F2A	91.7(19)	C2A[2]	C1A	N1	104.8(18)
F1A[2]	P1	F2A[1]	91.7(19)	C1A[1]	C2A	N1	131(2)
F1A	P1	F2A[2]	91.7(19)	N1	C3	C4	111.7(8)
F1A	P1	F2A	178(2)	N1	C3	C5	113.3(8)
F1A[1]	P1	F2A[1]	178(2)	N1	C3	C4A	111.2(17)
F1A	P1	F2A[1]	88.4(18)	N1	C3	C5A	107.7(15)
F1A[2]	P1	F2A	88.4(18)	C4	C3	C5	106.3(10)
F1A[1]	P1	F2A[2]	88.4(18)	C4A	C3	C5A	132(2)
F2A[2]	P1	F2A[1]	90.2(19)	N2	C6	Ni1	173.4(10)
F2A[2]	P1	F2A	90.2(19)	N2	C7	C8	106.7(13)
F2A[1]	P1	F2A	90.2(19)	N2	C7	C9	107.9(10)
F3	P2	F3[3]	91.3(6)	N2	C7	C10	101.3(12)
F3[4]	P2	F3[3]	91.3(6)	N2	C7	C8A	100.9(15)
F3	P2	F3[4]	91.3(6)	N2	C7	C9A	110.4(14)
F4[3]	P2	F3	81.3(7)	N2	C7	C10A	111.4(17)
F4[4]	P2	F3[4]	93.3(7)	C8	C7	C9	113.2(11)
F4	P2	F3[4]	81.3(7)	C8	C7	C10	114.6(11)
F4[4]	P2	F3	171.3(8)	C9	C7	C10	112.1(12)
F4[3]	P2	F3[3]	93.3(7)	C9A	C7	C8A	110.2(13)
F4	P2	F3	93.3(7)	C9A	C7	C10A	113.8(14)
F4[4]	P2	F3[3]	81.3(7)	C10A	C7	C8A	109.4(14)

Figure S18. Projection view with 50% probability ellipsoids:

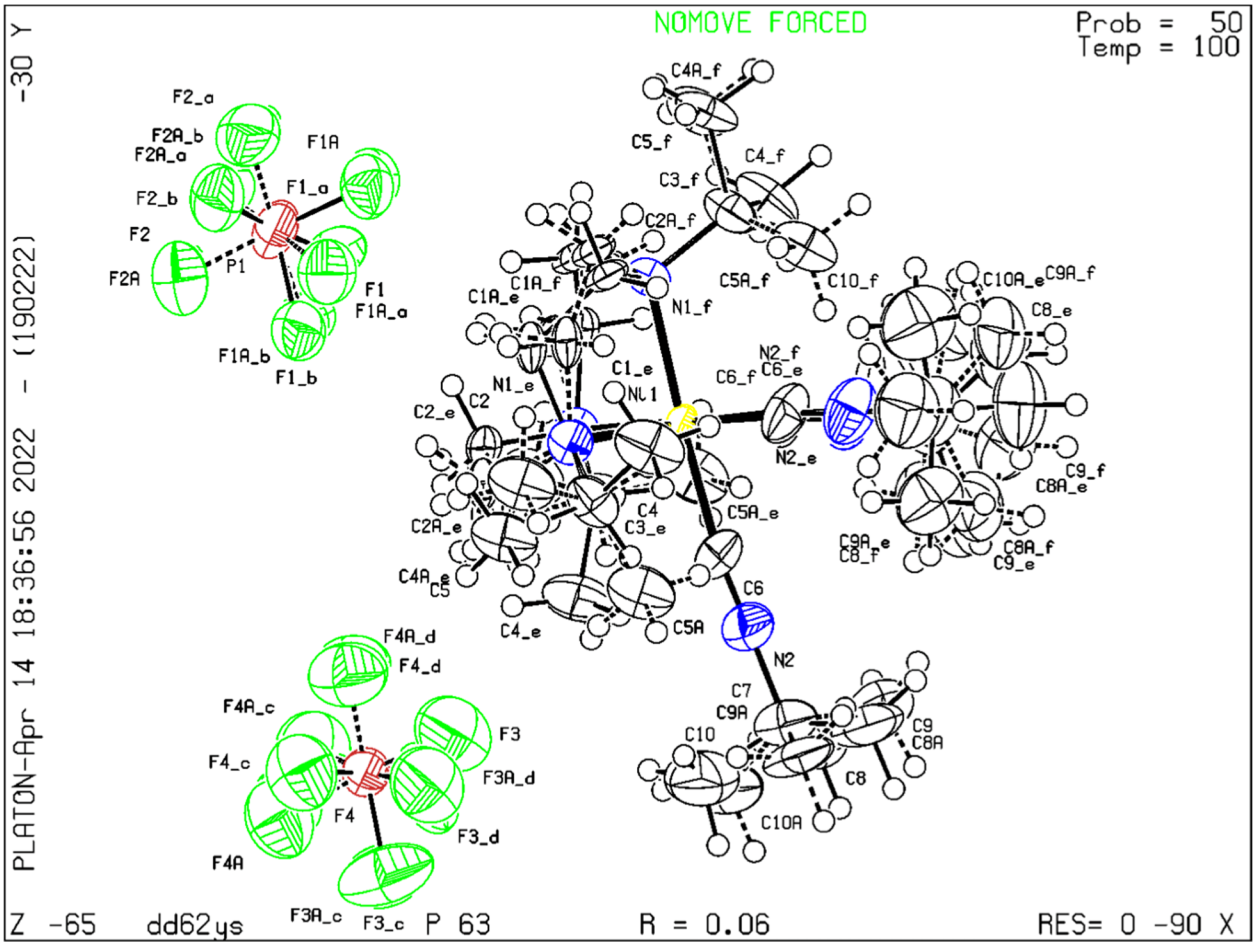
NOMOVE FORCED
Prob = 50
Temp = 100
PLATON-Apr 14 18:36:56 2022 - (190222)
-30 Y
Z -65
dd62ys
P 63
R = 0.06
RES= 0 -90 X
F2_a
F2A_b
F2A_a
F1A
F1_a
F2_b
F2
F2A
P1
F1
F1A_a
F1A_b
F1_b
C4A_f
C5_f
C4_f
C3_f
C2A_f
C1A_f
C1A_e
C5A_f
C10_f
N1_f
C10A_e
C9A_f
C8_e
N2_f
C6_f
C6_e
C1_e
N1_e
C2
C2_e
Ni1
N2_e
C9_f
C8A_e
C4
C3_e
C5A_e
C2A_e
C9A_e
C8_f
C8A_f
C9_e
C4A_e
C5
C4_e
C5A
C6
N2
C7
C9A
C10
C9
C8A
C8
C10A
F4A_d
F4_d
F4A_c
F3
F4_c
F3A_d
F4
F3_d
F4A
F3A_c
F3_c

[(iPr$_3$TACN)Ni^I(CN^{t}Bu)$_2$](PF$_6$) (5)

Table S15. Crystal data and structure refinement for [(iPr$_3$TACN)Ni^I(CN^{t}Bu)$_2$](PF$_6$).

Identification code	[iPrTACNNi(CNtBu)2]PF6
Empirical formula	$C_{25}H_{51}F_6N_5NiP$
Formula weight	625.38
Temperature/K	100.0
Crystal system	monoclinic
Space group	$P2_1/c$
a/Å	10.6246(4)
b/Å	19.0632(6)
c/Å	15.7487(5)
α/°	90
β/°	93.8780(10)
γ/°	90
Volume/Å^3	3182.42(19)
Z	4
ρ_{calc}g/cm^3	1.305
μ/mm^{-1}	0.717
F(000)	1332.0
Crystal size/mm^3	0.113 × 0.094 × 0.055
Radiation	MoKα (λ = 0.71073)
2Θ range for data collection/°	4.97 to 50.714
Index ranges	$-12 \le h \le 12$, $-22 \le k \le 22$, $-18 \le l \le 18$
Reflections collected	58756
Independent reflections	5821 [R_{int} = 0.0577, R_{sigma} = 0.0251]
Data/restraints/parameters	5821/0/355
Goodness-of-fit on F^2	1.036
Final R indexes [I>=2σ (I)]	R_1 = 0.0388, wR_2 = 0.0880
Final R indexes [all data]	R_1 = 0.0510, wR_2 = 0.0942
Largest diff. peak/hole / e Å^{-3}	0.55/-0.37

Table S16. Bond Lengths for [(iPr$_3$TACN)Ni^I(CN^{t}Bu)$_2$](PF$_6$).

Atom	Atom	Length/Å	Atom	Atom	Length/Å
Ni1	N1	2.2044(19)	C7	C8	1.524(4)
Ni1	N2	2.195(2)	C9	C10	1.525(4)
Ni1	N3	2.198(2)	C9	C11	1.532(3)
Ni1	C1	1.854(3)	C12	C13	1.520(3)
Ni1	C2	1.933(3)	C12	C14	1.532(4)
N1	C3	1.482(3)	C15	C16	1.512(5)
N1	C8	1.490(3)	C15	C17	1.535(4)

N1	C9	1.507(3)	C18	C19	1.510(4)
N2	C4	1.484(3)	C18	C20	1.525(4)
N2	C5	1.487(3)	C18	C21	1.515(4)
N2	C12	1.503(3)	C22	C23	1.521(4)
N3	C6	1.492(4)	C22	C24	1.517(3)
N3	C7	1.477(3)	C22	C25	1.504(4)
N3	C15	1.508(3)	P1	F1	1.585(2)
N4	C1	1.166(3)	P1	F2	1.6026(18)
N4	C18	1.462(3)	P1	F3	1.563(2)
N5	C2	1.151(3)	P1	F4	1.5832(18)
N5	C22	1.448(3)	P1	F5	1.591(2)
C3	C4	1.524(3)	P1	F6	1.571(2)
C5	C6	1.512(4)			

Table S17. Bond Angles for [(iPr_3TACN)$Ni^{I}(CN^{t}Bu)_2$](PF_6).

Atom	Atom	Atom	Angle/°	Atom	Atom	Atom	Angle/°
N2	Ni1	N1	82.86(7)	N1	C8	C7	111.9(2)
N2	Ni1	N3	83.79(8)	N1	C9	C10	111.8(2)
N3	Ni1	N1	80.77(7)	N1	C9	C11	114.3(2)
C1	Ni1	N1	97.81(9)	C10	C9	C11	110.6(2)
C1	Ni1	N2	133.44(10)	N2	C12	C13	110.7(2)
C1	Ni1	N3	142.55(10)	N2	C12	C14	115.0(2)
C1	Ni1	C2	87.63(11)	C13	C12	C14	110.9(2)
C2	Ni1	N1	174.34(9)	N3	C15	C16	112.0(2)
C2	Ni1	N2	92.29(10)	N3	C15	C17	113.2(3)
C2	Ni1	N3	95.85(9)	C16	C15	C17	109.9(3)
C3	N1	Ni1	101.16(14)	N4	C18	C19	107.4(2)
C3	N1	C8	111.32(19)	N4	C18	C20	108.1(2)
C3	N1	C9	109.59(18)	N4	C18	C21	107.9(2)
C8	N1	Ni1	109.87(14)	C19	C18	C20	109.9(3)
C8	N1	C9	112.23(19)	C19	C18	C21	112.0(2)
C9	N1	Ni1	112.17(14)	C21	C18	C20	111.4(3)
C4	N2	Ni1	107.87(15)	N5	C22	C23	107.1(2)
C4	N2	C5	112.47(19)	N5	C22	C24	107.9(2)
C4	N2	C12	113.1(2)	N5	C22	C25	106.7(2)
C5	N2	Ni1	100.58(15)	C24	C22	C23	111.8(2)
C5	N2	C12	110.10(19)	C25	C22	C23	111.5(2)
C12	N2	Ni1	112.03(14)	C25	C22	C24	111.6(2)
C6	N3	Ni1	106.33(15)	F1	P1	F2	89.56(12)
C6	N3	C15	109.9(2)	F1	P1	F5	87.55(15)
C7	N3	Ni1	105.31(15)	F3	P1	F1	177.53(15)

C7	N3	C6	111.1(2)	F3	P1	F2	89.72(13)
C7	N3	C15	111.6(2)	F3	P1	F4	90.63(14)
C15	N3	Ni1	112.46(17)	F3	P1	F5	90.08(15)
C1	N4	C18	166.7(3)	F3	P1	F6	90.34(15)
C2	N5	C22	175.5(3)	F4	P1	F1	90.08(13)
N4	C1	Ni1	169.8(2)	F4	P1	F2	179.60(12)
N5	C2	Ni1	168.5(2)	F4	P1	F5	90.67(11)
N1	C3	C4	113.07(19)	F5	P1	F2	89.13(11)
N2	C4	C3	112.79(19)	F6	P1	F1	92.03(15)
N2	C5	C6	113.2(2)	F6	P1	F2	90.20(11)
N3	C6	C5	113.9(2)	F6	P1	F4	90.00(11)
N3	C7	C8	111.6(2)	F6	P1	F5	179.21(12)

Figure S19. Projection view with 50% probability ellipsoids:

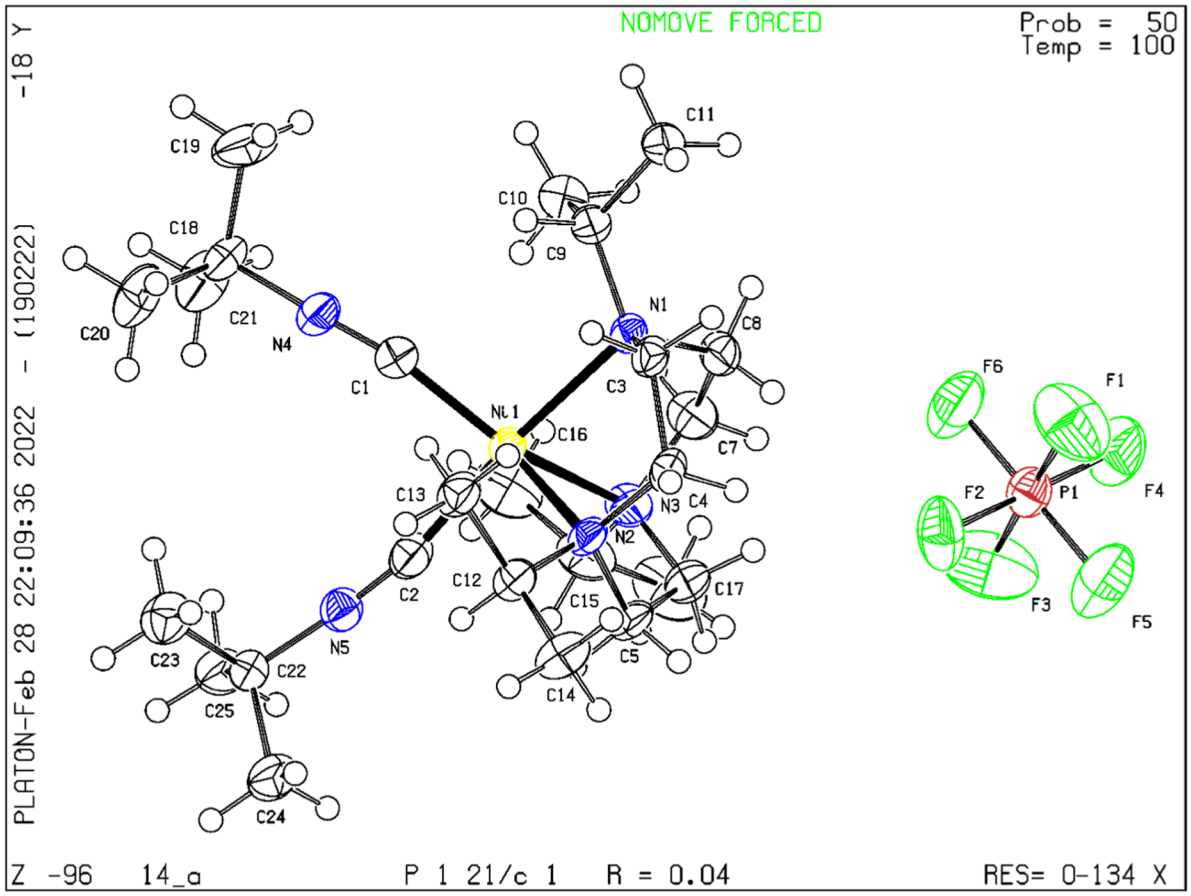

X. References

1. D. A. Valyaev, S. Clair, L. Patrone, M. Abel, L. Porte, O. Chuzel and J. L. Parrain, *Chem. Sci.*, 2013, **4**, 2815-2821.
2. C. A. Barta, S. R. Bayly, P. W. Read, B. O. Patrick, R. C. Thompson and C. Orvig, *Inorg. Chem.*, 2008, **47**, 2280-2293.
3. G. Haselhorst, S. Stoetzel, A. Strassburger, W. Walz, K. Wieghardt and B. Nuber, *J. Chem. Soc., Dalton Trans.*, *Dalton Trans.*, 1993, **1**, 83-90.
4. L. Griego, J. Chae and L. M. Mirica, manuscript submitted.
5. D. F. Evans, *J. Chem. Soc.*, 1959, 2003-2005.
6. J. Loliger and R. Scheffold, *J. Chem. Educ.*, 1972, **49**, 646-647.
7. A. W. Addison, T. N. Rao, J. Reedijk, J. van Rijn and G. C. Verschoor, *J. Chem. Soc., Dalton Trans.*, 1984, 1349-1356.
8. L. Yang, D. R. Powell and R. P. Houser, *Dalton Trans.*, 2007, **9**, 955-964.
9. J. N. Rebilly, G. Charron, E. Riviere, R. Guillot, A. L. Barra, M. D. Serrano, J. van Slageren and T. Mallah, *Chem. Eur. J.*, 2008, **14**, 1169-1177.
10. J.-N. Rebilly, L. Catala, E. Rivière, R. Guillot, W. Wernsdorfer and T. Mallah, *Inorg. Chem.*, 2005, **44**, 8194-8196.
11. M. J. Frisch, G. W. Trucks, H. B. Schlegel, G. E. Scuseria, M. A. Robb, J. R. Cheeseman, G. Scalmani, V. Barone, G. A. Petersson, H. Nakatsuji, X. Li, M. Caricato, A. V. Marenich, J. Bloino, B. G. Janesko, R. Gomperts, B. Mennucci, H. P. Hratchian, J. V. Ortiz, A. F. Izmaylov, J. L. Sonnenberg, Williams, F. Ding, F. Lipparini, F. Egidi, J. Goings, B. Peng, A. Petrone, T. Henderson, D. Ranasinghe, V. G. Zakrzewski, J. Gao, N. Rega, G. Zheng, W. Liang, M. Hada, M. Ehara, K. Toyota, R. Fukuda, J. Hasegawa, M. Ishida, T. Nakajima, Y. Honda, O. Kitao, H. Nakai, T. Vreven, K. Throssell, J. A. Montgomery Jr., J. E. Peralta, F. Ogliaro, M. J. Bearpark, J. J. Heyd, E. N. Brothers, K. N. Kudin, V. N. Staroverov, T. A. Keith, R. Kobayashi, J. Normand, K. Raghavachari, A. P. Rendell, J. C. Burant, S. S. Iyengar, J. Tomasi, M. Cossi, J. M. Millam, M. Klene, C. Adamo, R. Cammi, J. W. Ochterski, R. L. Martin, K. Morokuma, O. Farkas, J. B. Foresman and D. J. Fox, *Gaussian 16 Rev. B.01*, 2016, Gaussian, Inc., Wallingford CT.
12. Y. Zhao and D. G. Truhlar, *Theor. Chem. Acc.*, 2008, **120**, 215-241.
13. A. Schafer, H. Horn and R. Ahlrichs, *J. Chem. Phys.*, 1992, **97**, 2571-2577.
14. A. Schafer, C. Huber and R. Ahlrichs, *J. Chem. Phys.*, 1994, **100**, 5829-5835.
15. B. J. Shields, B. Kudisch, G. D. Scholes and A. G. Doyle, *J. Am. Chem. Soc.*, 2018, **140**, 3035-3039.
16. S. I. Ting, S. Garakyaraghi, C. M. Taliaferro, B. J. Shields, G. D. Scholes, F. N. Castellano and A. G. Doyle, *J. Am. Chem. Soc.*, 2020, **142**, 5800-5810.
17. Skripnikov, L. Chemissian, version 4.67, 2020 (www.chemissian.com, accessed March 2021).
18. Bruker, *Madison, Wisconsin, USA*, 2018.
19. L. Krause, R. Herbst-Irmer, G. M. Sheldrick and D. Stalke, *J. Appl. Crystallogr.*, 2015, **48**, 3-10.
20. G. Sheldrick, *Acta Cryst. A*, 2015, **71**, 3-8.
21. O. V. Dolomanov, L. J. Bourhis, R. J. Gildea, J. A. K. Howard and H. Puschmann, *J. Appl. Crystallogr.*, 2009, **42**, 339-341.
22. G. M. Sheldrick, *Acta Cryst.*, 2008, **A64**, 112-122.